

LEGIBILITY NOTICE

A major purpose of the Technical Information Center is to provide the broadest dissemination possible of information contained in DOE's Research and Development Reports to business, industry, the academic community, and federal, state and local governments.

Although a small portion of this report is not reproducible, it is being made available to expedite the availability of information on the research discussed herein.

CONF - 8710712 - 1

Los Alamos National Laboratory is operated by the University of California for the United States Department of Energy under contract W-7405-ENG-36

LA-UR--87-439

DE87 006056

TITLE: A Method for Treating Hourglass Patterns

AUTHOR(S): L. G. Margolin and J. J. Pyun

SUBMITTED TO: Fourth International Conference on "Numerical Methods in Laminar and Turbulent Flow," Montreal, Quebec, Canada, July 6-10, 1987

DISCLAIMER

This report was prepared as an account of work sponsored by an agency of the United States Government. Neither the United States Government nor any agency thereof, nor any of their employees, makes any warranty, express or implied, or assumes any legal liability or responsibility for the accuracy, completeness, or usefulness of any information, apparatus, product, or process disclosed, or represents that its use would not infringe privately owned rights. Reference herein to any specific commercial product, process, or service by trade name, trademark, manufacturer, or otherwise does not necessarily constitute or imply its endorsement, recommendation, or favoring by the United States Government or any agency thereof. The views and opinions of authors expressed herein do not necessarily state or reflect those of the United States Government or any agency thereof.

By acceptance of this article, the publisher recognizes that the U.S. Government retains a nonexclusive, royalty-free license to publish or reproduce the published form of this contribution, or to allow others to do so, for U.S. Government purposes.

The Los Alamos National Laboratory requests that the publisher identify this article as work performed under the auspices of the U.S. Department of Energy.

Los Alamos Los Alamos National Laboratory
Los Alamos, New Mexico 87545

[Handwritten signature]

A METHOD FOR TREATING HOURGLASS PATTERNS

L. G. Margolin
Lawrence Livermore National Laboratory
Livermore, California 94550, USA

J. J. Pyun
Los Alamos National Laboratory
Los Alamos, New Mexico, 87545, USA

ABSTRACT

We have developed a new scheme to identify and suppress hourglass patterns. The scheme has been incorporated into a two-dimensional (2D) Lagrangian hydrodynamic (hydro) code, and extensive calculations have been performed to demonstrate the effectiveness of our treatment.

Hourglassing is a problem frequently encountered in numerical simulations of fluid and solid dynamics. The problem arises because certain volume-preserving distortions of cell shape produce no restoring forces. The result is an unrestricted drifting mode in the velocity field that leads to severe distortions of the computational mesh. These distortions cause large errors in the numerical approximations of the equations of motion. The drift may also allow adjacent vertices to get very close to each other. This results in the computational time step based on a Courant stability condition to become very small, effectively halting the calculation.

We describe a mathematical formalism that identifies and selectively damps the hourglass patterns. The damping is constructed to preserve the physical aspects of the solution while maintaining a reasonable computational mesh. We further describe the implementation of our scheme in a 2D hydro code, and show the relative improvement in the results of six different test problems that we calculated.

1. INTRODUCTION

Hourglassing is a problem frequently encountered in

numerical simulations of fluid and solid dynamics. The problem arises because certain volume-preserving distortions of cell shape produce no restoring forces. In a Lagrangian calculation, where the cell vertices move with the local material velocity, the result is an unrestrained drifting mode that leads to severe distortion of the mesh. The hourglassing distortion in particular causes large errors in the numerical approximations of spatial gradients in the equations of motion (1). The drift may also allow adjacent vertices on the mesh to get very close to each other. This causes the computational time step based on a Courant stability condition to become very small, effectively halting the calculation.

An hourglass velocity pattern is shown in Fig. 1-a for a regular mesh, where velocities are calculated and stored at cell vertices. At a later time shown in Fig. 1-b, the mesh has deformed. However, the volume of each cell is unchanged in time. Consequently, the density remains constant in each cell and no work has been done. Since pressure depends only on density and internal energy, the pressure field is also unchanged. Thus this velocity pattern produces no restoring forces and will persist, leading ultimately to a bowtied mesh. On more irregular mesh, we can decompose a general velocity field into a sum of independent patterns, one of which represents hourglassing. The key feature of an hourglass pattern is a global deformation that does not change the volume of any cell. We shall show that the existence of such a pattern is a topological property of the mesh - i.e., of cells having four sides - and does not depend on the details of the differencing scheme.

Physically, the continuum equations of motion are well-posed, which means that there are exactly as many equations as unknowns. In the process of discretization, this balance has been upset. On a quadrilateral cell, the degrees of freedom exceed the constraints. In section 2, we review the modes of motion of a 2D quadrilateral cell and we identify the number of degrees of freedom associated with the motion of such a

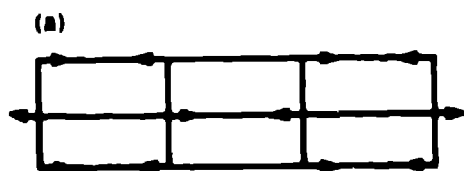


Fig. 1(a) An initially rectangular mesh with an hourglass velocity pattern

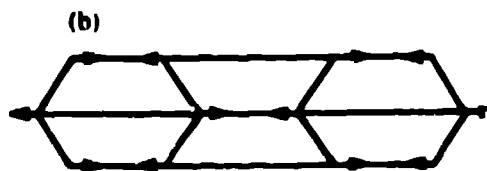


Fig. 1(b) The same mesh at a later time. The motion has produced no restoring forces. The motion will continue unrestrained and will eventually cause bowtied cells

cell. Then we develop a simple mathematical formalism to identify and selectively damp the hourglassing modes in section 3. The particular form of the filter depends on the details of the differencing scheme. In section 4 we exhibit one realization of the filter for a common choice of spatial differencing (2). Our filter is local, explicit and remarkably effective. In section 5 we discuss results of six pairs of calculations. In each pair, one with the filter and the other without, we show that the mesh is considerably improved in the filtered calculations resulting in considerably reduced problem running times. We also compare the physical solutions in each pair to show that the filter does not alter the solution in any aspect that can be considered physical.

2. MODES OF CELL MOTION

We consider a typical quadrilateral computational cell in Fig. 2. In a two-dimensional geometry, such a cell has eight degrees of freedom, that is, a vertical velocity (V) and a horizontal velocity (U) for each of the four vertices.

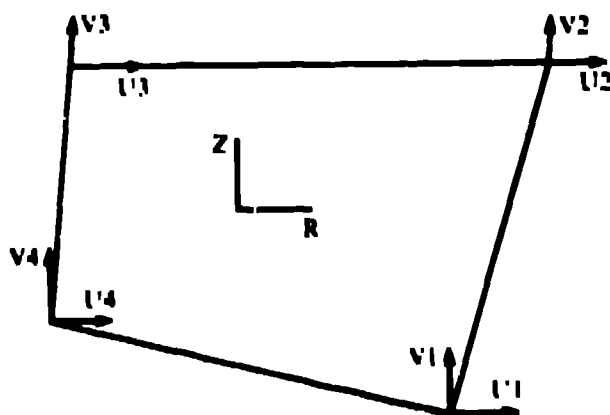


Fig 2 A quadrilateral computational cell

Instead of considering the individual components, we can consider patterns made up of parts of the velocities of several vertices in Fig. 3. These patterns are equivalent to the degrees of freedom; again there are eight independent patterns.

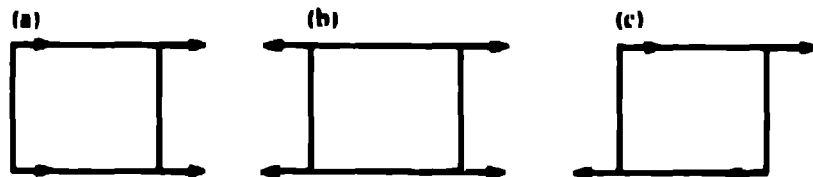


Fig. 3. Some patterns of cell motion (a) uniform horizontal translation, (b) horizontal strain and (c) shear

We identify the physical patterns in the following way. Any physical motion that changes the shape or volume of a cell should produce a restoring force. Conversely, any cell deformation that produces no restoring force is nonphysical. Nonphysical cell deformation is exemplified by the hourglassing.

Allowing for spatially constant strains in a cell, we can identify six of the patterns with physical modes of motion and also with mathematical objects. The physical modes are

- one pattern of horizontal translation
- one pattern of vertical translation
- one pattern of rotation
- one pattern of horizontal strain
- one pattern of vertical strain
- one pattern of shear strain

The restoring forces in a solid are stresses that arise because of strains. The strains are the time integrals of strain rates. The strain rates are just the spatial gradients of velocity. Therefore, we identify the six degrees of freedom with the six mathematical objects

$$\bar{U}, \bar{V}, \partial U/\partial x, \partial U/\partial y, \partial V/\partial x, \text{ and } \partial V/\partial y \quad . \quad (1)$$

3. MATHEMATICAL FORMALISM FOR THE FILTER

To construct a mathematical formalism for the filter that expresses these ideas, we begin by considering an eight-dimensional vector space. The velocity components of the cell vertices can be represented as vector in this space

$$\vec{V} = (U_1, U_2, U_3, U_4, V_1, V_2, V_3, V_4) \quad (2)$$

The six degrees of freedom can now be represented in terms of vector operators in this space. For example, if the uniform motion \bar{U} of a cell (the degree of freedom associated horizontal translational invariance) is defined as

$$\bar{U} = .25^* (U_1 + U_2 + U_3 + U_4) \quad (3)$$

then a vector operator \vec{L}_1 can be defined so that

$$\bar{U} = \vec{L}_1 \cdot \vec{V} \quad (4)$$

Here $\vec{L}_1 = .25^* (1, 1, 1, 1, 0, 0, 0, 0)$ and the dot represents the inner product of the vectors.

The velocity gradients are also linear forms in the vertex velocities and can be expressed as inner products. We define the vector $\vec{L}_1, \vec{L}_2, \vec{L}_3, \vec{L}_4, \vec{L}_5$, and \vec{L}_6 , by

$$\bar{U} = \vec{L}_1 \cdot \vec{V} \quad \bar{V} = \vec{L}_2 \cdot \vec{V}$$

$$\begin{aligned}
\partial U / \partial x &= \vec{L}_3 \cdot \vec{V} & \partial V / \partial x &= \vec{L}_4 \cdot \vec{V} \\
\partial U / \partial y &= \vec{L}_5 \cdot \vec{V} & \partial V / \partial y &= \vec{L}_6 \cdot \vec{V}
\end{aligned} \tag{5}$$

A specified realization of the vectors will be given in the example that follows in the next section. At this point, it is important to realize that the vectors depend only on the particular form of the difference approximations used in the code.

The vectors \vec{L}_1 through \vec{L}_6 correspond to the physical degrees of freedom of the cell. However, they do not completely span the eight-dimensional vector space of possible modes of cell motion. There are two additional vectors, \vec{L}_7 and \vec{L}_8 , required to span the space. These are easily constructed by requiring them to be orthogonal to the set \vec{L}_1 through \vec{L}_6 , and to each other. The patterns \vec{L}_7 and \vec{L}_8 correspond to motions that deform the cell and yet do not produce restoring forces. By our definition, they are the nonphysical modes and in fact correspond to the hourglass patterns.

We are now prepared to take the final step. By selectively filtering the modes proportional to \vec{L}_7 and \vec{L}_8 , we can eliminate the hourglassing without altering any of the forces in the calculation. Now the eight operators \vec{L}_1 through \vec{L}_8 are a linearly independent set, and so span the eight-dimensional space of possible velocity vectors. Also any vector in this space can be expanded in a complete set

$$\vec{V} = \sum (\vec{L}_j \cdot \vec{V}) \vec{L}_j \quad j=1, 2, \dots, 6 \tag{6}$$

$$\vec{V} = \vec{V} - [(\vec{L}_7 \cdot \vec{V})\vec{L}_7 + (\vec{L}_8 \cdot \vec{V})\vec{L}_8] \alpha \tag{7}$$

Here, α represents the fraction of the hourglassing that we filter from the velocity field on each cycle. The vectors \vec{L}_7 and \vec{L}_8 are chosen to have unit length.

α is a dimensionless number that can be thought of as the ratio of the time step Δt to a relaxation time τ_r . The inverse of α is the number of computational cycles to achieve complete relaxation. Since each vertex is shared by four cells, and the filter is applied separately to each of these, complete relaxation in one cycle would mean choosing $\alpha = .25$. Larger values than .25 would overcorrect and lead to instability. However there are other reasons to choose even smaller values of α .

In our analysis, we have treated the cell as if it existed in isolation from the rest of the mesh. However the effects of filter applied separately to each cell do overlap since each node is shared by four cells. Since the hourglassing is a global pattern in which cell volumes do not change, it is clear that the unconstrained degrees of freedom are not two per cell, but only two for the entire mesh. The

superposition of filtering for each cell approximates a single filter for the entire mesh.

In practice, the boundary and corner nodes are filtered two times and one time respectively, whereas the filter is applied to the inner nodes four times. This filtering process is efficiently done by using a fully-vectorized DO loop which sweeps the cells in the radial direction first and then proceeds to the axial direction for a cylindrical geometry.

The effectiveness of the filter is due to the way in which corrections from the four cells sharing a node interact. Qualitatively, they reinforce each other for the part of the hourglassing that is global and tend to cancel each other for other parts of the the global velocity field. To enhance this cancellation, it is important that alpha be chosen to be constant over the entire mesh, rather than varying from cell to cell. Also, we have tried allowing alpha to vary from cycle to cycle, but find this is not as effective, nor as easily implemented, as simply fixing alpha for the entire calculation.

Because the filter is only approximate, we should use as small a value of alpha as is sufficient to control the hourglassing deformation. A full answer to how small alpha can be chosen would require a detailed understanding of the source of the hourglassing. Practically speaking, we have found choosing alpha in the range

$$.01 < \alpha < .05$$

works for most calculations.

4. A SPECIFIC RELIZATION OF THE FILTER

Consider a typical spatial differencing for a mesh of irregular quadrilateral cells in cylindrical geometry (2). For the translational terms we choose

$$\begin{aligned}\bar{U}/\bar{R} &= (U_1+U_2+U_3+U_4)/(R_1+R_2+R_3+R_4) \\ \bar{V} &= 0.25 (V_1+V_2+V_3+V_4)\end{aligned}\tag{8}$$

For the spatial gradients, we use

$$\begin{aligned}\partial U/\partial r &= [(U_1-U_3)(z_2-z_4) + (U_2-U_4)(z_3-z_1)]/2A \\ \partial U/\partial z &= [(U_1-U_3)(r_4-r_2) + (U_2-U_4)(r_1-r_3)]/2A \\ \partial V/\partial r &= [(V_1-V_3)(z_2-z_4) + (V_2-V_4)(z_3-z_1)]/2A \\ \partial V/\partial z &= [(V_1-V_3)(r_4-r_2) + (V_2-V_4)(r_1-r_3)]/2A\end{aligned}\tag{9}$$

where $2A = (r_2-r_4)(z_3-z_1) + (r_3-r_1)(z_4-z_3)$ is twice the area of the cell. By inspection, we write

$$\begin{aligned}\vec{L}_1 &= 0.25(1, 1, 1, 1, 0, 0, 0, 0) \\ \vec{L}_2 &= 0.25(0, 0, 0, 0, 1, 1, 1, 1) \\ \vec{L}_3 &= (z_2-z_4, z_3-z_1, z_4-z_2, z_1-z_3, 0, 0, 0, 0) \\ \vec{L}_4 &= (0, 0, 0, 0, z_2-z_4, z_3-z_1, z_4-z_2, z_1-z_3) \\ \vec{L}_5 &= (r_4-r_2, r_1-r_3, r_2-r_4, r_3-r_1, 0, 0, 0, 0) \\ \vec{L}_6 &= (0, 0, 0, 0, r_4-r_2, r_1-r_3, r_2-r_4, r_3-r_1)\end{aligned}\tag{10}$$

Then it is easy to verify that a (nonunique) choice for the hourglass vectors is

$$\begin{aligned}\vec{L}_7 &= 0.5(-1, 1, -1, 1, 0, 0, 0, 0) \\ \vec{L}_8 &= 0.5(0, 0, 0, 0, -1, 1, -1, 1)\end{aligned}\tag{11}$$

5. COMPARISON AND DISCUSSION OF TEST PROBLEMS

In verifying the effectiveness of our hourglass filter, we have run more than one hundred test problems with and without the filter. We will discuss the results of six typical problems in this section.

Test problem number one consist of a steel ball, and a concentric steel shell with a vacuum between them. Initially the inner ball has radius 0.5 cm. The shell has an inner radius of 1.0 cm and an outer radius of 2.0 cm. The ball is stationary and the shell is imploded spherically with a constant velocity of 100 cm/ms. The shell collides with the ball at approximately 0.0027 ms. Then the ball and shell rebound together as shown in Fig. 4. The interface between the ball and shell is treated as a free slip surface after collision. Figure 4-a shows that the hourglass filter prevents appreciable hourglassing and also stabilizes the slip interface. Figure 4-b, calculated without the filter, shows classical hourglass patterns. Free slip interfaces seem to be especially susceptible to hourglassing, probably because the nodes on the interface have fewer constraints.

The filtered calculation better preserves the spherical symmetry expected in the calculation. However, the average radius of each sphere of nodes (representing Lagrangian points in the material) is identical in both calculations, supporting our claim that the hourglass filter does not alter the physical aspects of the solution.

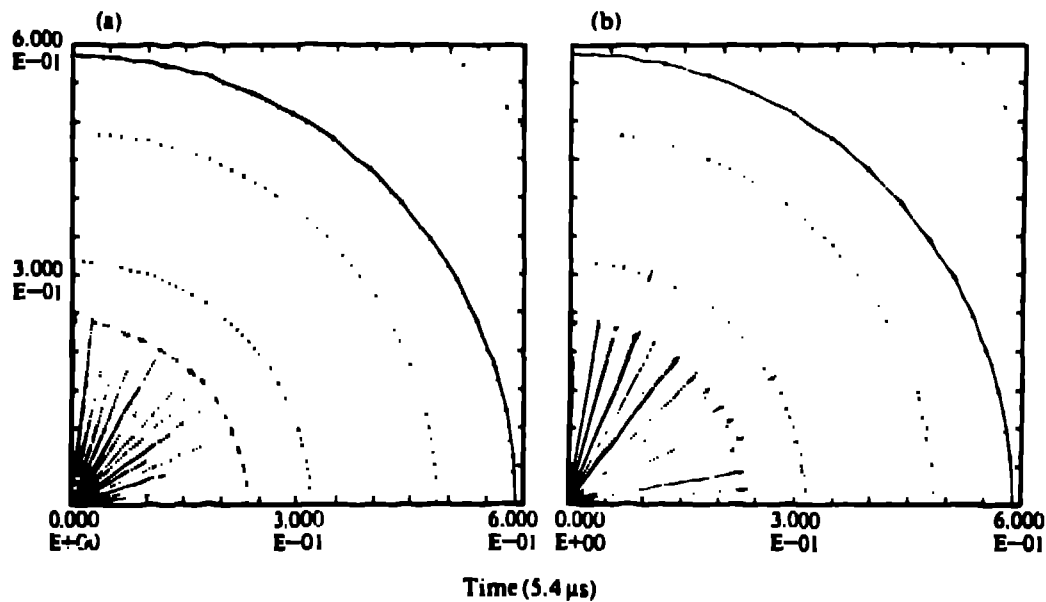


Fig. 4. Calculations of collision and rebound of two steel balls with (a) and without (b) filter

Test problem number two consists of three concentric steel shells initially in contact with each other. A weak shock of about 3 Kbars is generated in the middle shell along a 45 degree line from the polar (vertical) axis. The shock moves azimuthally toward the equator where it is reflected at about 0.02 ms. The two interfaces between shells are treated as free slip surfaces. Figure 5-a shows that the filter eliminates the hourglass patterns. The position of the interfaces is identical in both calculations.

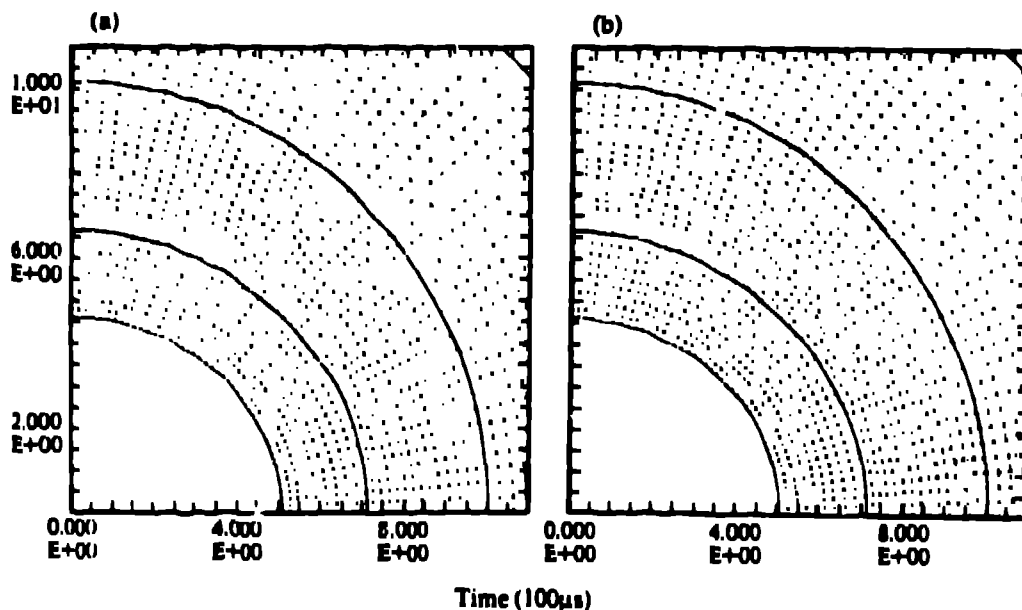


Fig. 5. Calculations of azimuthal shock with (a) and without (b) filter

Test problem number three is a shaped charge with a copper liner. The shaped charge is a cylinder with an outer radius of 7 cm and with a height of 24 cm. The average thickness of the copper liner is 0.5 cm and its inner radius is approximately 5.5 cm. The explosive is detonated at time zero. Figure 6 shows part of the copper liner being accelerated by the explosive at 0.045 ms. Figure 6-b shows hourglass patterns along the polar axis, and the same time a bowtied mesh in the tail section of the liner. There are no bowties and no hourglass patterns in the filtered calculation shown in Fig. 6-a.

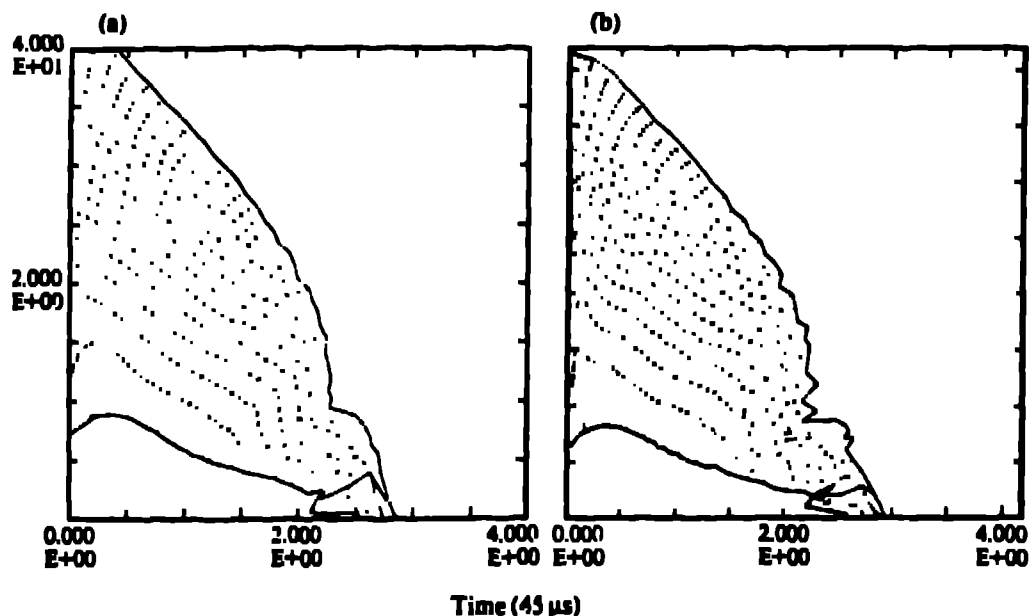


Fig. 6. Calculations of shaped charge with (a) and without (b) filter

Test problem number four consists of three coaxial cylinders. The upper and lower cylinders are identical. They are made of steel, 0.6 cm in radius and 0.5 cm thick. Sandwiched between them is a smaller cylinder made of copper. The copper cylinder is 0.1 cm both in radius and thickness. The steel cylinders move axially toward each other with a relative velocity of 0.5 cm/ms. The copper disk is squeezed and extrudes radially into the air gap. Hourglass patterns are prominently visible along an interface between the copper disk and the air gap in Fig. 7-b. No hourglass patterns are manifest in Fig. 7-a when the filter is employed.

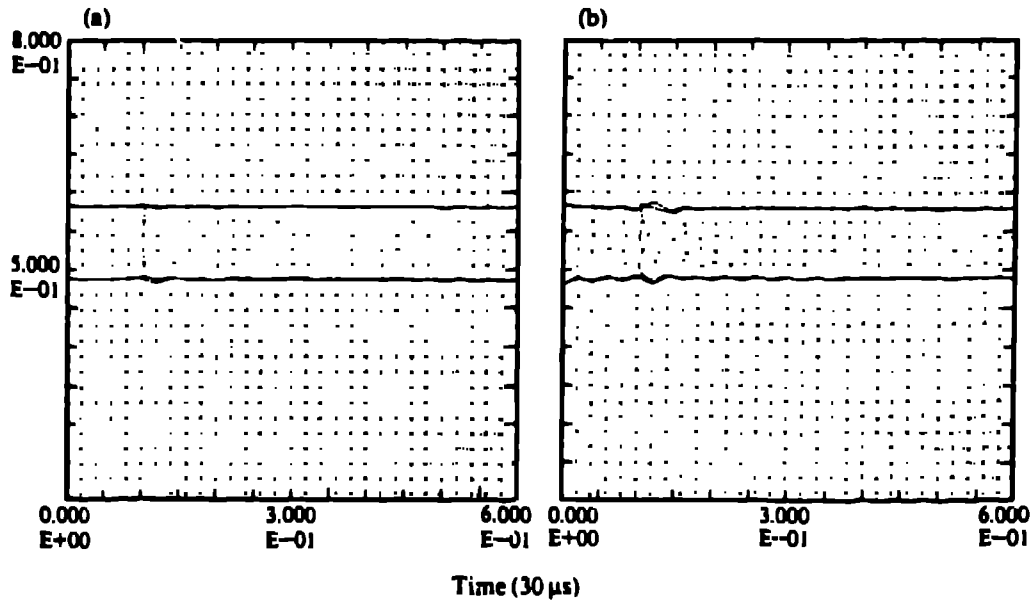


Fig. 7. Calculations of copper disk under compression with (a) and without (b) filter

Test problem number five simulates the impact of a solid steel ball with alluvium. Alluvium is a relatively weak geologic material. The alluvium is initially a (nearly) infinite plane representing a river bed. The steel ball has an initial radius of 5 cm. The steel ball impacts the alluvium vertically with a velocity of 500 cm/ms. Figure 8 shows the penetration of the ball into the alluvium. No conspicuous hourglass patterns are visible even in Fig. 8-b. However, the hourglass filter has clearly eliminated a mesh instability along the slip line in Fig. 8-a.

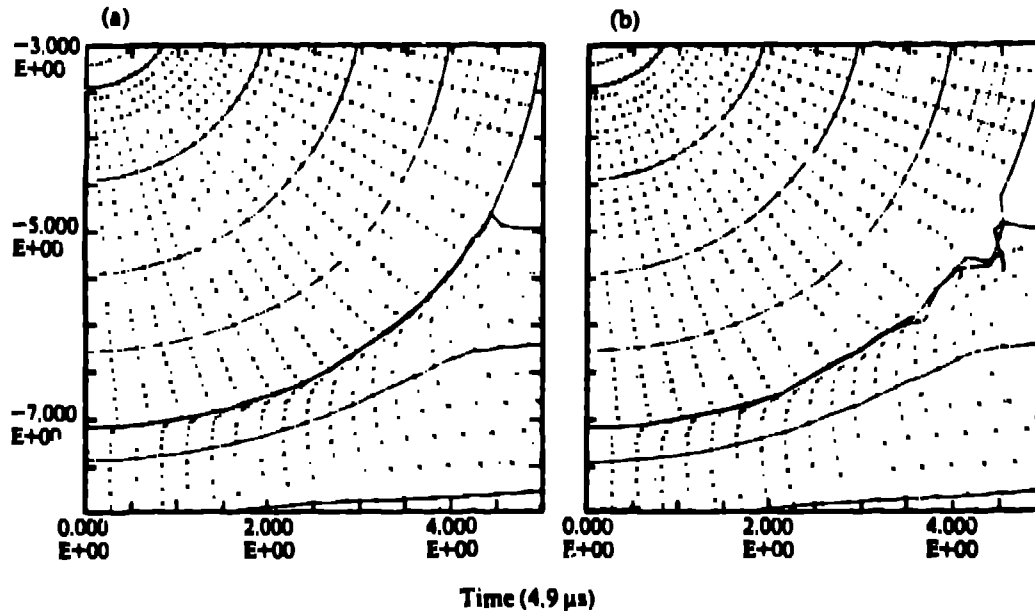


Fig. 8. Calculations of collision between steel ball and alluvium river bed with (a) and without (b) filter

The final test problem, number six, shows a steel disk with rigidly constrained boundaries. A strong plane shock (approximately 8 Mbars) is generated on the top boundary and moves vertically downward to the bottom boundary where it is reflected. In Fig. 9-b, the unfiltered calculation shows extensive mesh distortion due to hourglassing. The filtered calculation in Fig. 9-a exhibits a clean and regular mesh, maintaining the expected physical symmetry of the material motion.

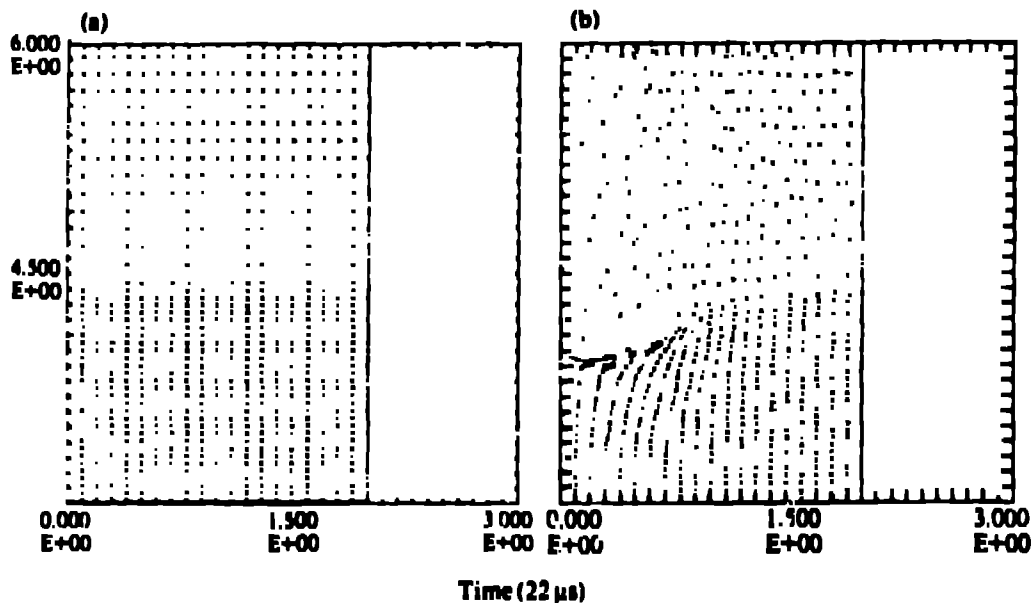


Fig. 9. Calculations of plane shock in steel with (a) and without (b) filter

None of the test problems in this section have analytic solutions. However, we have compared physical aspects of solutions between the filtered and the unfiltered calculations. These aspects include the position of material interfaces, shock velocities and the jumps in physical variables across the shocks. The results of these comparisons indicate that the hourglassing filter does not change the physical solution if the value of α , the dimensionless ratio of time step Δt to relaxation time τ_r , is less than 0.06.

One benefit of using the hourglass filter is the often large decrease in cycles and hence CPU (central processing unit) time to complete a calculation. Table 1 lists a comparison of running times for the six test problems with and without the filter. The saving in CPU time varies from 0 to

75 percent. This saving is associated with the higher time step that is allowed with a more regular mesh. For example, 4850 cycles are required to run test problem number one to a time of 0.0055 ms in the unfiltered calculation whereas only 950 are required when the filter is used.

Table 1

Comparison of Running CPU (central processor unit)
Time (s) in Cray X-MP Computer

Test Problem Number	Problem Time (ms)	CPU Time or with filter	(Cycles) without filter	CPU Time Saving (percent)
1	0.0055	41(950)	163(4850)	75
2	0.1	84(721)	84(721)	0
3	0.0507	208(1660)	281(32250)	26
4	0.03	293(2299)	324(2580)	10
5	0.005	161(336)	534(1849)	70
6	0.023	357(1500)	500(7647)	29

6. REFERENCES

1. Margolin, L.G. and Tarwater, A.E., "A Diffusion Operator for Lagrangian Meshes," Proceedings, the 5th International Conference on Numerical Methods in Thermal Problems, Montreal, Canada, June, 1987 (to be published).
2. Margolin, L.G. and Adams, T.F., "Spatial Differencing for Finite Difference Codes," Los Alamos National Laboratory Report LA-10249, January, 1981.